Research Square

Preprints are preliminary reports that have not undergone peer review.
They should not be considered conclusive, used to inform clinical practice,
or referenced by the media as validated information.

Modelling of Reaction Between Magnetite and Uranium Under Beishan Groundwater Conditions

Wanqiang Zhou

zhouwqpku@163.com

Tongling University

Research Article

Keywords: Magnetite, Uranium, Reaction, Groundwater, Geochemical modeling

Posted Date: August 24th, 2026

DOI: https://doi.org/10.21203/rs.3.rs-10697473/v1

License: This work is licensed under a Creative Commons Attribution 4.0 International License. Read Full License

Additional Declarations: No competing interests reported.

Abstract

The reaction between radionuclides and minerals is critical for the safe disposal of high-level radioactive waste. This study investigated the reaction pathways between magnetite and uranium in Beishan groundwater using the PHREEQC software. The results demonstrate that magnetite can effectively reduce U(VI), with the resulting U(IV) then precipitating as uraninite. However, at low uranium concentrations, the U(IV) generated by reduction is insufficient to drive uraninite precipitation. Increased temperatures enhance the reduction of U(VI) by magnetite and promote uraninite precipitation, thereby decreasing uranium mobility. The selection of thermodynamic database significantly influences the U(VI) reduction by magnetite.

1. Introduction

Currently, a deep geological repository (DGR) based on the “multi-barrier” concept is regarded as the most suitable strategy for the safe disposal of high-level radioactive waste (HLW) worldwide [1]. Under this approach, solidified HLW is encased in canisters and deposited in deep geological rock at depths of 500–1,000 meters underground. However, the service life of an HLW repository is on the order of tens of thousands of years. If the canisters are damaged during storage, there is a risk that the contained radionuclides will migrate and disperse into the groundwater, posing a threat to the environment and human health. Consequently, a comprehensive safety assessment of the repository must be conducted during the site selection. This assessment must include the reactions between radionuclides and minerals in the barrier system, as these constitute a key component of the overall safety assessment [2–5].

The Beishan area of Gansu Province has been identified as a priority candidate site for China’s deep geological repository for HLW. The nation’s first underground research laboratory for the geological disposal of HLW is currently under construction in this region. While studies have investigated the speciation of radionuclides in Beishan groundwater and their adsorption behaviour on mineral surfaces, few have modelled the redox reactions occurring between radionuclides and minerals [6–9]. Previous studies have reported that iron minerals can significantly limit the mobility of radionuclides through sorption, coprecipitation and reduction processes in repository environments [10–14]. Magnetite is a mixed ferric and ferrous oxide that is widely found in geological environments. It is also the main corrosion product of waste canisters intended for the long term disposal [12, 15].

Uranium is a redox-sensitive element capable of existing in multiple valence states [16]. Under well-oxidized conditions, uranium predominantly occurs in the hexavalent state, generally present as uranyl complexes in groundwater, and exhibits relatively high mobility. In contrast, under anoxic and reducing conditions, uranium primarily exists in the tetravalent state, typically as crystalline precipitates, and displays considerably lower mobility. Magnetite contains divalent iron and possesses a certain reducing capacity [17, 18]. Studying the reaction between magnetite and uranium is important for predicting the long-term stability of DGR and assessing the effectiveness of the barrier system in retaining radionuclides.

PHREEQC is a powerful geochemical modelling software developed by the U.S. Geological Survey [19]. It has become one of the most widely used computational tools in the fields of water-rock interaction, radionuclide transport and environmental remediation [20]. Significant advantages of the software include its open-source and free nature, concise input syntax, and comprehensive database. PHREEQC has been successfully applied in areas such as safety assessments of geological repositories, the prediction of sorption behavior and the study of the

migration of radionuclides. Chen et al. [21] used PHREEQC software to calculate the saturation index of insoluble minerals in relation to the uranium extraction process and the chemical composition of leaching at a uranium deposit. Li et al. [22] used this software to predict the natural attenuation capability of sandstone aquifers at uranium mining sites and the surrounding areas. Mühr-Ebert et al. [23] compared experimental results and PHREEQC calculations to evaluate the speciation of uranium in groundwaters. Reiller et al. [24] studied the aqueous speciation of uranium and radium in mining acidic waters based on time-resolved laser-induced fluorescence spectroscopy (TRLFS) and PHREEQC modelling.

This work aims to use PHREEQC to simulate reaction pathways between magnetite and U(VI) using groundwater from the Beishan area as a case study. The effects of different uranium concentrations, temperatures and databases on the reactions will be analysed, as will the theoretical effectiveness of magnetite in inhibiting uranium mobility. The goal is to provide theoretical references and data support for the safety assessment of DGR in China.

2. Principles of simulation

Reaction path simulation is a forward modeling approach in geochemistry, grounded in thermodynamic equilibrium theory, that tracks the progressive evolution of a system's chemical composition as a function of "reaction progress" (e.g., titrant addition) in response to external perturbations. The underlying concept is to decompose complex geochemical reactions into a series of sequential equilibrium states; by computing the chemical equilibrium at each step, the complete evolutionary pathway from the initial to the final state of the system can be reconstructed. This approach is conceptually analogous to a laboratory experiment in which reactants are incrementally added to a reaction vessel while the resulting changes are monitored.

Given the known chemical composition of groundwater at the starting point, the reaction path simulation method employs a mass-balance model to determine the extent of water-rock interactions and the mass transfer of minerals, thereby predicting the final chemical composition of the aqueous phase. This constitutes a forward modeling problem. PHREEQC calculates chemical equilibria by solving a system of multivariate nonlinear equations, based on mass-balance equations, the law of mass action, and charge-balance constraints.

In this work, the LLNL database of PHREEQC (Version 3.7.3) was employed. This database originates from the thermodynamic dataset compiled by the Lawrence Livermore National Laboratory (LLNL) for the EQ3/6 and GWB software packages, and has been reformatted for compatibility with PHREEQC. Among all standard databases distributed with PHREEQC, the LLNL database features one of the most comprehensive coverages of elements and aqueous species, rendering it particularly suitable for handling complex groundwater systems containing multiple trace components [25].

To better adapt to the reducing environment characteristic of the repository, the reaction system in this study was modeled as a closed system. The initial uranium concentration was set to 1.0×10^{-4} mol/L, with uranium present in the hexavalent state. The groundwater utilized in this work is from Beishan borehole BS28 at depths ranging from 365 to 900 meters, which is adjacent to the site of China's first underground research laboratory currently under construction for the HLW repository and is thus considered representative. Yang et al. [26] reported a pH of 8.1 and an Eh of 98 mV for this groundwater; the detailed chemical composition is presented in Table 1. Magnetite was added incrementally to the groundwater at a total dosage ranging from 0 to 0.02 mol/L, in 20 equal steps of 1 mmol/L per addition.

Table 1
Chemical compositions of groundwaters in the Beishan area (mmol/L).

Components	Na^+	Ca^{2+}	K^+	Mg^{2+}	Cl^-	HCO_3^-	SO_4^{2-}	F^-	NO_3^-	pH	*Eh*(mV)
Concentration	45.2	4.58	0.409	2.08	36.2	2.15	9.18	0.106	0.228	7.8	98

3. Results and discussion

3.1 Redox reaction of magnetite with U(VI)

The redox reaction between magnetite and U(VI) is illustrated in Fig. 1. At magnetite concentrations below 4 mmol/L, U(VI) reduction is challenging, and its aqueous concentration remains unchanged. It is evident that as the magnetite concentration is increased further, there is a rapid decline in the aqueous U(VI) concentration. When the mineral concentration attains 10 mmol/L, it can be deduced that approximately 90% of the U(VI) in the system has been reduced to U(IV). Consequently, the U(VI) concentration declines in a gradual manner with an increase in magnetite content, ultimately reaching a state of stability at approximately 2.4×10^{-6} mol/L. The findings of this study suggest that magnetite has the capacity to markedly reduce the mobility of uranium through a process of reductive transformation.

During the reaction of magnetite with U(VI), the system pH increases progressively with rising magnetite concentration, evolving from an initial value of 7.8 to 9.8. This pH elevation is attributable to the consumption of H^+ ions in the groundwater solution by the dissolution of magnetite and the concomitant reduction reactions. Simultaneously, hydrolysis of dissolved Fe(II)/Fe(III) species following magnetite dissolution alters the carbonate buffering system, thereby further contributing to the pH increase. The introduction of magnetite as a reducing agent into the Beishan groundwater solution results in a decrease in the pe value from 1.66 to − 3.65, which corresponds to an Eh decline from 98 mV to − 216 mV. The transition of Eh from positive to negative values is indicative of a shift in the groundwater environment from oxidizing to reducing conditions.

The saturation index (SI) is a logarithmic measure that quantifies the degree of deviation of an aqueous solution from mineral equilibrium. This provides a thermodynamic indication of the tendency for mineral dissolution or precipitation. When SI < 0, the mineral is undersaturated and tends to dissolve; when SI > 0, the mineral is supersaturated and tends to precipitate; when SI = 0, the mineral is exactly at equilibrium with respect to dissolution and precipitation. This study examined the variations in the saturation indexes of uraninite and schoepite as a function of increasing magnetite concentration under Beishan groundwater conditions, as presented in Fig. 1b. The results show that in the absence of magnetite addition, the SI of uraninite is − 0.62, indicating that precipitation of this mineral does not occur in the system. With progressive addition of magnetite, the SI of uraninite shifts from negative to positive values and eventually rises to 5.36, suggesting that hexavalent uranium is gradually reduced to tetravalent uraninite, which subsequently precipitates, thereby continuously diminishing uranium mobility. Prior to magnetite addition, the SI of schoepite is − 0.42, and throughout the entire reaction process, the SI of schoepite remains negative, indicating that schoepite precipitation is thermodynamically unfavorable. It is noteworthy that the SI of schoepite exhibits an initial increase followed by a subsequent decrease as the reaction proceeds. This behavior can be attributed to the rapid pH rise from 7.8 to 9.5 during the early stage of magnetite reaction. Under elevated pH conditions, the increased OH^- concentration drives the transformation of dissolved uranyl species into schoepite precipitate ($UO_3{\cdot}2H_2O$). Subsequently, as the

magnetite concentration continues to increase, the pe decreases substantially, leading to extensive reduction of U(VI) to U(IV) and a marked decline in UO_2^{2+} concentration, which in turn causes the SI of schoepite to decrease progressively.

3.2 Reduction of U(VI) at low concentrations

The present study investigates the effect of lower uranium concentrations on the reductive reaction of uranium by magnetite. To this end, the reduction and immobilisation behaviour of uranium by magnetite was examined at an initial uranium concentration of 1.0×10^{-10} mol/L, and the results were compared with those obtained at a higher concentration (1.0×10^{-4} mol/L).

The reaction between magnetite and U(VI) at low concentration is presented in Fig. 2a. At magnetite concentrations below 4 mmol/L, the U(VI) concentration remains essentially unchanged, indicating that U(VI) reduction is ineffective during this stage. It is evident that as the magnetite concentration increases, the aqueous U(VI) concentration undergoes a rapid decline. It is noteworthy that when the magnetite concentration attains ~ 8 mmol/L, the preponderance of U(VI) in the system has been significantly reduced. Consequently, the U(VI) concentration declines in a gradual manner with an increase in magnetite content, ultimately reaching a state of stability at approximately 2.5×10^{-12} mol/L. The reduction trend of U(VI) at low concentrations is highly similar to that at high concentrations, with a notable decline occurring at approximately 4 mmol/L of magnetite in both cases, and the final residual U(VI) fractions are comparable (2.5%–3%). The variations in system pH and pe are demonstrated in Fig. 2c and 2d. The trends in pH and pe evolution are almost identical to those observed at high concentrations. This indicates that the redox state and acid-base properties of the system are predominantly governed by the intrinsic characteristics of magnetite itself.

The variations in the SI of uraninite and schoepite as a function of magnetite concentration are shown in Fig. 2b. Prior to magnetite addition, the SI of schoepite is approximately − 6.5, and throughout the entire reaction process, the SI of schoepite remains negative, indicating that schoepite precipitation is thermodynamically unfavorable. In the absence of magnetite addition, the SI of uraninite is approximately − 6.7. With increasing magnetite concentration in the system, the SI of uraninite gradually rises from negative values but ultimately approaches only − 0.64, never transitioning to positive values. This stands in marked contrast to the high concentration condition, in which the SI of uraninite increases to 5.36, indicating the sustained formation of substantial uraninite precipitates. The persistent undersaturation of uraninite under low concentration conditions can be attributed to the following reason: although magnetite can effectively reduce U(VI) to U(IV), the total uranium concentration is extremely low (1.0×10^{-10} mol/L), and the resulting U(IV) concentration remains far below the solubility product of uraninite, insufficient to drive the nucleation and precipitation of this mineral. Consequently, under low concentration conditions, uranium persists in the aqueous phase as dissolved U(IV) species.

Latta et al. [27] investigated the adsorption and reduction of U(VI) by titanium-substituted magnetite, and found that U(VI) could be reduced by Fe(II) present in the mineral. However, analysis of the EXAFS spectra of the reaction products revealed no contribution from U-U interactions. This finding indicates that the reduction products were not tetravalent uranium precipitates but rather tetravalent uranium surface complexes. In a subsequent study, the same research team examined the structural products of U(VI) reduction by magnetite under varying uranium concentrations and found that uraninite was formed at higher uranium concentrations, whereas tetravalent uranium surface complexes were generated at lower concentrations [28]. These findings are in good agreement with the simulation results, which demonstrate that U(VI) is reduced to uraninite under high

concentration conditions, while under low concentration conditions it remains in the aqueous phase as dissolved U(IV), which is susceptible to adsorption onto mineral surfaces [29].

3.3 Effect of temperature on the redox reaction

Temperature is a critical parameter affecting thermodynamic equilibrium of geochemical reactions. In the context of deep geological disposal, the temperature of groundwater may be elevated due to the release of radiogenic heat from HLW. This elevated temperature could, in turn, affect the reductive reaction of uranium by magnetite and the precipitation behavior of uranium minerals. The present study investigated the reductive reaction of U(VI) by magnetite, and the saturation indexes of schoepite and uraninite under different temperature conditions (25°C, 45°C, and 65°C).

The reaction between magnetite and U(VI) are presented in Fig. 3a (linear scale) and 3b (logarithmic scale). The overall trends in U(VI) concentration as a function of magnetite concentration are generally consistent across the three temperatures. As demonstrated in Fig. 3b, an increase in magnetite concentration beyond 8 mmol/L results in a concomitant rise in the residual U(VI) concentration, with the highest observed at 25°C, followed by 45°C, and the lowest at 65°C. This finding suggests that elevated temperatures promote the reductive reaction of U(VI) by magnetite, thereby enhancing uranium removal efficiency. At a magnetite concentration of 20 mmol/L, the residual U(VI) concentration is approximately 2.87×10^{-6} mol/L at 25°C, 1.84×10^{-6} mol/L at 45°C, and decreases to approximately 1.25×10^{-6} mol/L at 65°C. It is noteworthy that in the initial stage at relatively low magnetite concentrations, the three curves nearly overlap, suggesting that the reduction reaction is primarily governed by the available magnetite supply, and the temperature effect has not yet fully manifested.

The variation in the saturation index of schoepite as a function of magnetite concentration and temperature is depicted in Fig. 3c. At 45°C, the trend in schoepite SI is analogous to that at 25°C, yet it exhibits a higher peak value that exceeds zero, indicating that elevated temperature favours schoepite precipitation. A more pronounced effect is observed at 65°C: the schoepite SI has an initial value of 0.02, increases rapidly to 0.84 with rising magnetite concentration, and remains above zero throughout the magnetite concentration range of 0–12 mmol/L. This indicates that at 65°C, schoepite is supersaturated over a broad range of magnetite concentrations and exhibits a strong tendency to precipitate. The variation in the saturation index of uraninite as a function of magnetite concentration and temperature is demonstrated in Fig. 3d. The trends in uraninite SI are nearly identical across the three temperatures: in the absence of magnetite addition, the SI of uraninite is relatively low, with values of − 0.62 at 25°C, − 0.11 at 45°C, and − 1.74 at 65°C; with increasing magnetite concentration, the SI rises rapidly, stabilises at ~ 8 mmol/L, and ultimately remains around 5.3. This result indicates that once the magnetite concentration reaches a critical threshold, uraninite enters a state of strong supersaturation, and the degree of supersaturation does not vary significantly with further increases in magnetite concentration. This finding indicates that temperature exerts a negligible influence on the long-term saturation state of uraninite, and that the final SI is predominantly influenced by the total uranium concentration and the redox potential of the system, rather than by temperature.

In summary, the effects of temperature on the reductive reaction of uranium by magnetite and the precipitation behavior of uranium minerals exhibit notable distinctions. It has been demonstrated that elevated temperatures enhance the reduction efficiency of U(VI), implying that magnetite exhibits a greater capacity for reduction and retardation of uranium in higher temperature conditions. Furthermore, elevated temperatures have been observed to promote the formation of hexavalent uranium as schoepite. However, the influence of temperature on uraninite

precipitation is comparatively minor. Indeed, uraninite precipitation is primarily governed by the total uranium concentration and the redox potential of the system, rather than by temperature.

3.4 Effect of thermodynamic database selection on the redox reaction

The SIT database is the only database within the PHREEQC software that employs the Specific Ion Interaction Theory (SIT). It is applicable to thermodynamic systems at low to moderate temperatures and medium-to-high ionic strengths, and holds significant application value in the fields of seawater geochemistry and radioactive waste disposal [30].

The results of the magnetite-U(VI) reaction, calculated using the SIT database, are presented in Fig. 4. In marked contrast to the results obtained with the LLNL database, the SIT database predicts that magnetite cannot effectively reduce U(VI) across the entire concentration range examined. As demonstrated in Fig. 4a, the total aqueous U(VI) concentration remains essentially constant at 1.0×10^{-4} mol/L, exhibiting no variation with increasing magnetite concentration. As demonstrated in Fig. 4b, an increase in magnetite concentration is accompanied by a gradual decrease in the system pe, from 1.66 to − 2.12, which corresponds to an Eh decline from 98 mV to − 125 mV. Despite the system manifesting a propensity towards enhanced reducing conditions, the magnitude of the pe decrease is considerably less than that calculated with the LLNL database, where pe decreases from 1.66 to − 3.65 and Eh drops from 98 mV to − 216 mV.

As demonstrated in Fig. 4c, the variation in U(VI) aqueous speciation as a function of magnetite concentration is illustrated, with the calculations being carried out using the SIT database. At low magnetite concentrations, the dominant species in solution are $Ca_2UO_2(CO_3)_3$ and $CaUO_2(CO_3)_3^{2-}$. As the magnetite concentration increases, the solution pH rises progressively. Concurrently, the concentrations of the aforementioned species gradually decrease, while the concentration of $(UO_2)_2(CO_3)(OH)_3^-$ increases markedly and becomes the predominant species after the magnetite concentration reaches 10 mmol/L. Furthermore, the concentrations of hydroxyl complexes, such as $UO_2(OH)_3^-$and $(UO_2)_3(OH)_7^+$, also increase slowly with rising pH values. As demonstrated in Fig. 4d, the U(VI) speciation calculated with the LLNL database differs considerably due to the absence of thermodynamic data for Ca–U(VI)–CO_3 ternary complexes within the database. The initially dominant species as determined by this database is $UO_2(CO_3)_3^{4-}$ and this decreases rapidly with increasing magnetite concentration, with all U(VI) species eventually approaching zero. As stated in previous research [31], the reduction process of uranium is not only related to the surface properties of minerals, but also closely associated with the aqueous speciation of uranium. When U(VI) exists as $CaUO_2(CO_3)_3^{2-}$ in solution, uranium adsorbed on mineral surfaces remains solely in the U(VI) form. This is in good agreement with the simulation results of the present study.

To summarize, the findings of this study indicate that the choice of thermodynamic database exerts a decisive influence on the prediction of U(VI) reduction behavior. In carbonate-buffered systems such as the Beishan groundwater, which contains Ca^{2+} and HCO_3^-, the differing treatments of the stability of Ca–U(VI)–CO_3 ternary complexes across various databases may lead to conclusions that are entirely contradictory. Consequently, in practical applications, the applicability of the selected database should be validated against experimental data, and sensitivity analyses should be performed with respect to the specific hydro-chemical conditions, so as to ensure the reliability of geochemical modelling results.

4. Conclusions

Based on the simulation results, the following conclusions can be drawn: (1) Magnetite can effectively reduce U(VI) in Beishan groundwater, and the resulting U(IV) precipitates as uraninite. (2) At low uranium concentrations, the reduction trend of U(VI) by magnetite is similar to that at high concentrations; however, owing to the extremely low total uranium content, the produced U(IV) is insufficient to drive the nucleation and precipitation of uraninite, and uranium instead remains in the aqueous phase as dissolved U(IV) species. (3) Elevated temperatures promote the reductive reaction of U(VI) by magnetite. Higher temperatures favor the supersaturation and precipitation of schoepite, but exert only a limited effect on the long-term saturation state of uraninite, whose formation is primarily governed by the total uranium concentration and the redox potential of the system. (4) The selection of thermodynamic database exerts a decisive influence on the prediction of U(VI) reduction behavior. In practical applications, the applicability of the selected database should be validated against experimental data, and database selection should be tailored to the specific conditions of the groundwater to ensure the reliability of the modeling results.

Declarations

Acknowledgements

Funding for this research was provided by Talent Research Start-up Fund of Tongling University (No. 2022tlxyrc20) and Natural Science Research Key Program of Tongling University (No. 2024tlxykjZD09).

Conflict of Interest statement

The authors declare that they have no known competing financial interests or personal relationships that could have appeared to influence the work reported in this paper.

References

1. R.C. Ewing, Long-term storage of spent nuclear fuel, Nature Mat., 14 (2015) 252.
2. J. Wang, L. Chen, R. Su, X. Zhao, The Beishan underground research laboratory for geological disposal of high-level radioactive waste in China: Planning, site selection, site characterization and in situ tests, J. Rock Mech. Geotech. Eng, 10 (2018) 411-435.
3. H. Geckeis, J. Lützenkirchen, R. Polly, T. Rabung, M. Schmidt, Mineral-water interface reactions of actinides, Chem. Rev., 113 (2013) 1016-1062.
4. P.L. Smedley, D.G. Kinniburgh, Uranium in natural waters and the environment: Distribution, speciation and impact, Appl. Geochem., 148 (2023) 105534.
5. B. Ma, L. Charlet, A. Fernandez-Martinez, M. Kang, B. Madé, A review of the retention mechanisms of redox-sensitive radionuclides in multi-barrier systems, Appl. Geochem., 100 (2019) 414-431.
6. W. Zhou, D. Xian, X. Su, Y. Li, W. Que, Y. Shi, J. Wang, C. Liu, Macroscopic and spectroscopic characterization of U(VI) sorption on biotite, Chemosphere, 255 (2020) 126942.
7. C. Wang, X. Yang, F. Wei, J. He, L. Qi, C. Liu, The influence of pH on diffusion of 75Se(IV) in Beishan granite, J. Radioanal. Nucl. Chem., 319 (2018) 365-377.

8. J. He, B. Ma, M. Kang, C. Wang, Z. Nie, C. Liu, Migration of (75)Se(IV) in crushed Beishan granite: Effects of the iron content, J. Hazard. Mater., 324 (2017) 564-572.
9. W. Zhou, X. Wang, C. Liu, Solubility, speciation and sorption calculation of americium in far-field and near-field Beishan groundwaters, J. Radioanal. Nucl. Chem., 334 (2025) 863-872.
10. B. Ma, M. Kang, Z. Zheng, F. Chen, J. Xie, L. Charlet, C. Liu, The reductive immobilization of aqueous Se(IV) by natural pyrrhotite, J. Hazard. Mater., 276 (2014) 422-432.
11. Z. Yang, M. Kang, B. Ma, J. Xie, F. Chen, L. Charlet, C. Liu, Inhibition of U(VI) reduction by synthetic and natural pyrite, Environ. Sci. Technol., 48 (2014) 10716-10724.
12. Y. Ma, X. Cheng, M. Kang, G. Yang, M. Yin, J. Wang, S. Gang, Factors influencing the reduction of U(VI) by magnetite, Chemosphere, 254 (2020) 126855.
13. L. Loreggian, J. Sorwat, J.M. Byrne, A. Kappler, R. Bernier-Latmani, Role of Iron Sulfide Phases in the Stability of Noncrystalline Tetravalent Uranium in Sediments, Environ. Sci. Technol., 54 (2020) 4840-4846.
14. Y. Kobayashi, K. Fukushi, S. Kosugi, A robust model for prediction of U(VI) adsorption onto ferrihydrite consistent with spectroscopic observations, Environ. Sci. Technol., 54 (2020) 2304-2313.
15. Z. Pan, B. Bartova, T. LaGrange, S.M. Butorin, N.C. Hyatt, M.C. Stennett, K.O. Kvashnina, R. Bernier-Latmani, Nanoscale mechanism of UO2 formation through uranium reduction by magnetite, Nat. Commun., 11 (2020) 4001.
16. K. Maher, J.R. Bargar, B.G. Jr, Environmental speciation of actinides, Inorg. Chem., 52 (2013) 3510-3532.
17. E.S. Ilton, J.-F. Boily, E.C. Buck, F.N. Skomurski, K.M. Rosso, C.L. Cahill, J.R. Bargar, A.R. Felmy, Influence of dynamical conditions on the reduction of UVI at the magnetite–solution interface, Environ. Sci. Technol., 44 (2010) 170-176.
18. Z. Pan, Y. Roebbert, A. Beck, B. Bartova, T. Vitova, S. Weyer, R. Bernier-Latmani, Persistence of the Isotopic Signature of Pentavalent Uranium in Magnetite, Environ. Sci. Technol., 56 (2022) 1753-1762.
19. D.L. Parkhurst, C.A.J. Appelo, User's guide to PHREEQC - a computer program for speciation,batch-reaction, one-dimensional transport, and inversegeochemical calculations, U.S. Geological Survey, Water-Resources Investigations Report, 312 (1999).
20. J.C. Bullen, O. Landa-Cansigno, D.J. Weiss, Teaching Adsorption Chemistry by Constructing Surface Complexation Models (SCM) in PHREEQC, J. Chem. Educ., 101 (2024) 1914-1924.
21. T. Chen, J. Liu, Y. Yang, J. Zhang, Q. Xu, L. Zhu, Study on precipitation and plugging mechanism in CO2 + O2 in-situ leaching of uranium in Nalinggou uranium deposit, J. Radioanal. Nucl. Chem., 333 (2024) 6283-6296.
22. C. Li, Q. Liu, L. Liu, Y. Li, X. Zhao, Z. Liu, Simulation of the natural attenuation of groundwater contaminated by acid in situ leaching at a uranium mine, J. Radioanal. Nucl. Chem., 333 (2024) 4907-4917.
23. E.L. Mühr-Ebert, F. Wagner, C. Walther, Speciation of uranium: Compilation of a thermodynamic database and its experimental evaluation using different analytical techniques, Appl. Geochem., 100 (2019) 213-222.
24. P.E. Reiller, P. L'Hermite, V. Plagnes, A. Jost, B. Reilé, M. Leermakers, M. Descostes, Speciation of uranium and radium during the treatment of acidic waters from legacy-mine (Le Cellier, France), Journal of Environmental Chemical Engineering, 13 (2025) 116289.
25. P. Lu, G. Zhang, J. Apps, C. Zhu, Comparison of thermodynamic data files for PHREEQC, Earth-Science Reviews, 225 (2022).

26. G. Yang, M. Kang, X. Cheng, Y. Ma, Y. Liu, J. Li, J. Wang, A novel methodology for investigating the redox potential of underground water in China's Beishan HLW repository site, J. Radioanal. Nucl. Chem., 322 (2019) 923-932.
27. D.E. Latta, C.I. Pearce, K.M. Rosso, K.M. Kemner, M.I. Boyanov, Reaction of U(VI) with titanium-substituted magnetite: influence of Ti on U(IV) speciation, Environ. Sci. Technol., 47 (2013) 4121-4130.
28. D.E. Latta, B. Mishra, R.E. Cook, K.M. Kemner, M.I. Boyanov, Stable U(IV) complexes form at high-affinity mineral surface sites, Environ. Sci. Technol., 48 (2014) 1683-1691.
29. Z. Wang, K.-U. Ulrich, C. Pan, D.E. Giammar, Measurement and Modeling of U(IV) Adsorption to Metal Oxide Minerals, Environmental Science & Technology Letters, 2 (2015) 227-232.
30. C.M. Lopez, P. Zhang, S.D. Favela, Y. Xiong, Y. Wang, Application of machine learning for modeling brønsted-guggenheim-scatchard specific ion interaction theory (SIT) coefficients, Appl. Geochem., 155 (2023) 105730.
31. D.M. Singer, S.M. Chatman, E.S. Ilton, K.M. Rosso, J.F. Banfield, G.A. Waychunas, Identification of simultaneous U(VI) sorption complexes and U(IV) nanoprecipitates on the magnetite (111) surface, Environ. Sci. Technol., 46 (2012) 3811-3820.

Figures

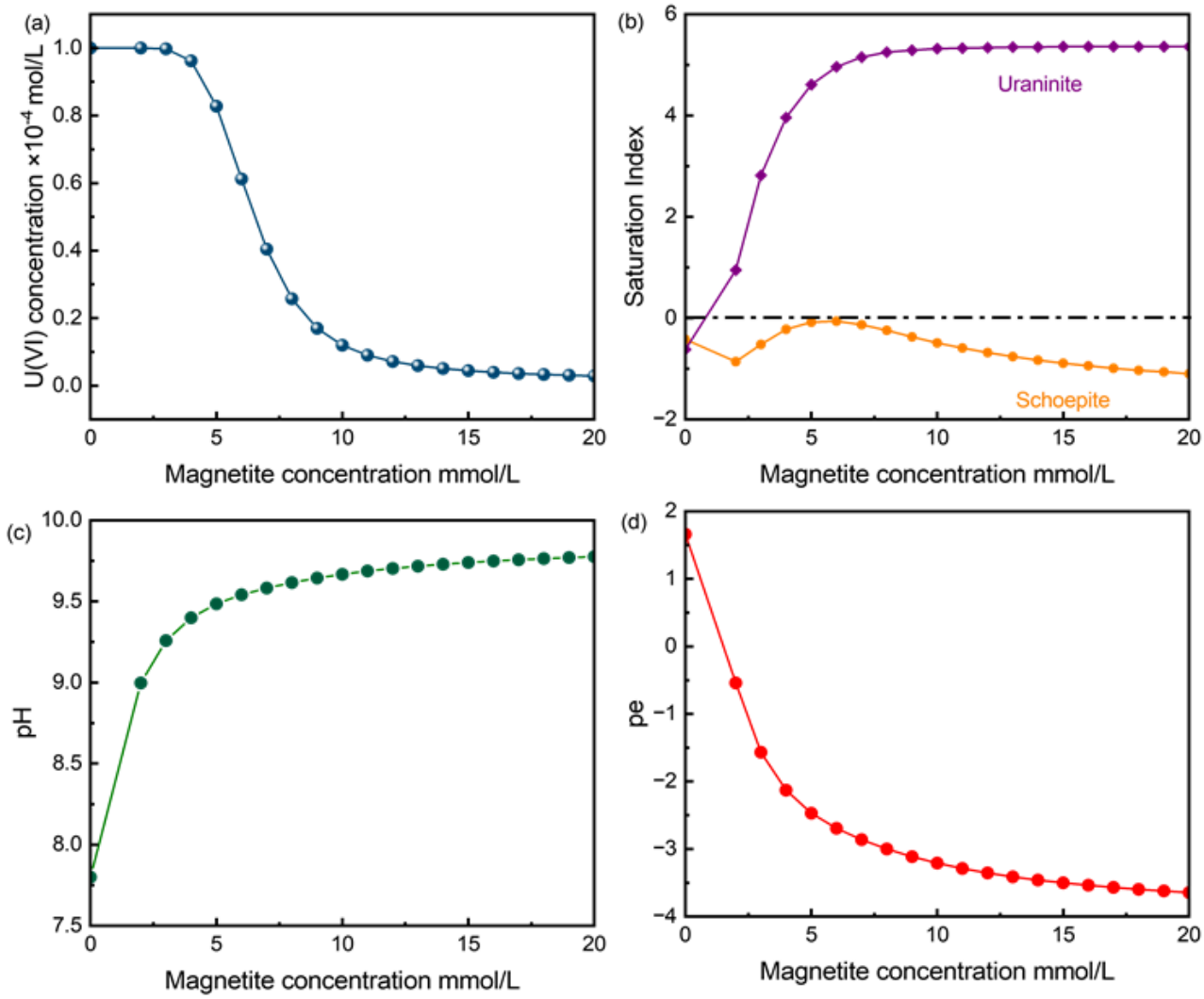


Figure 1

Trends of U(VI) concentration (a), saturation index of uranium minerals (b), pH (c) and pe (d) as a function of magnetite concentration (total uranium concentration: 1.0×10^{-4} mol/L)

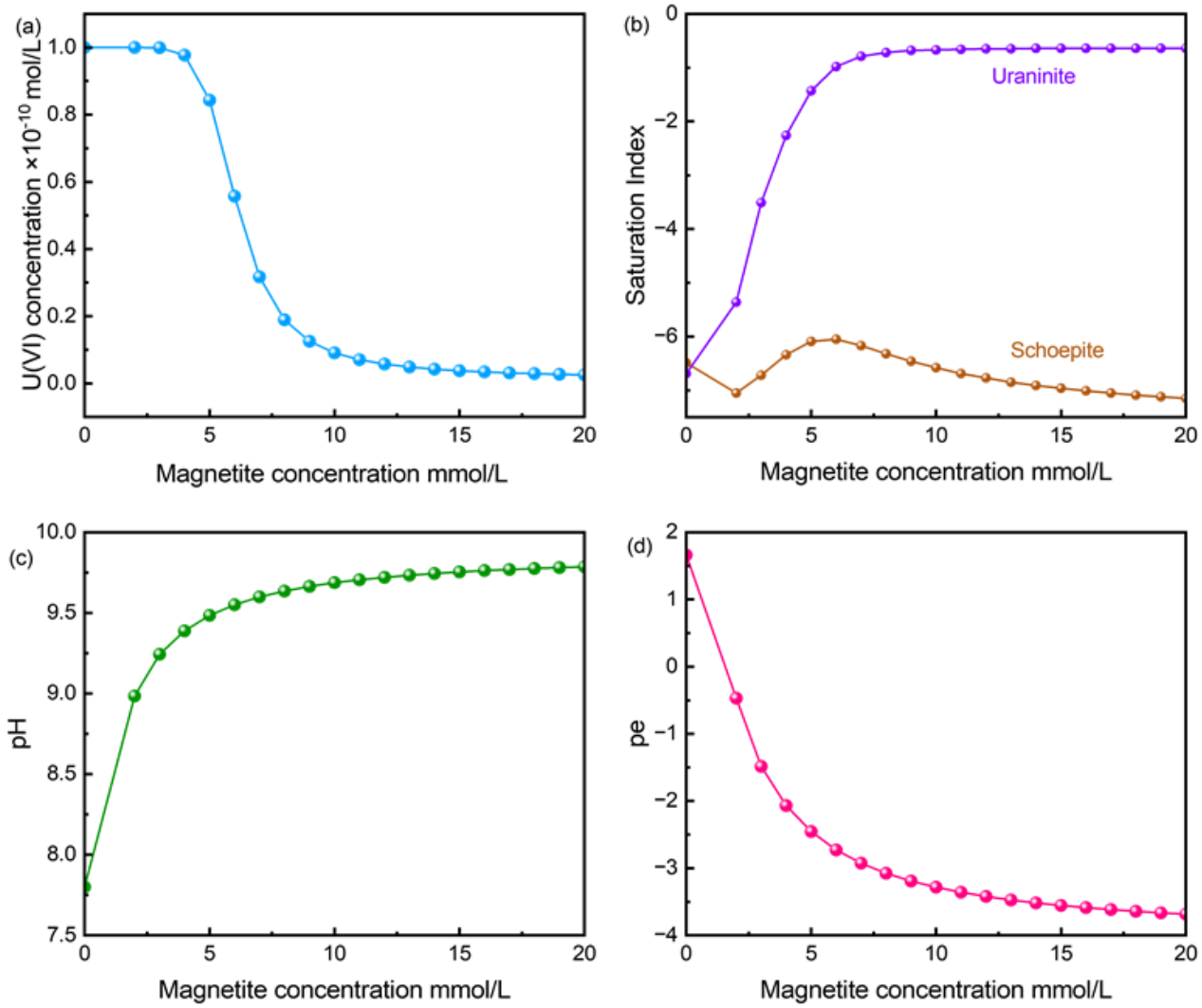


Figure 2

Trends of U(VI) concentration (a), saturation index of uranium minerals (b), pH (c) and pe (d) as a function of magnetite concentration (total uranium concentration: 1.0×10^{-10} mol/L)

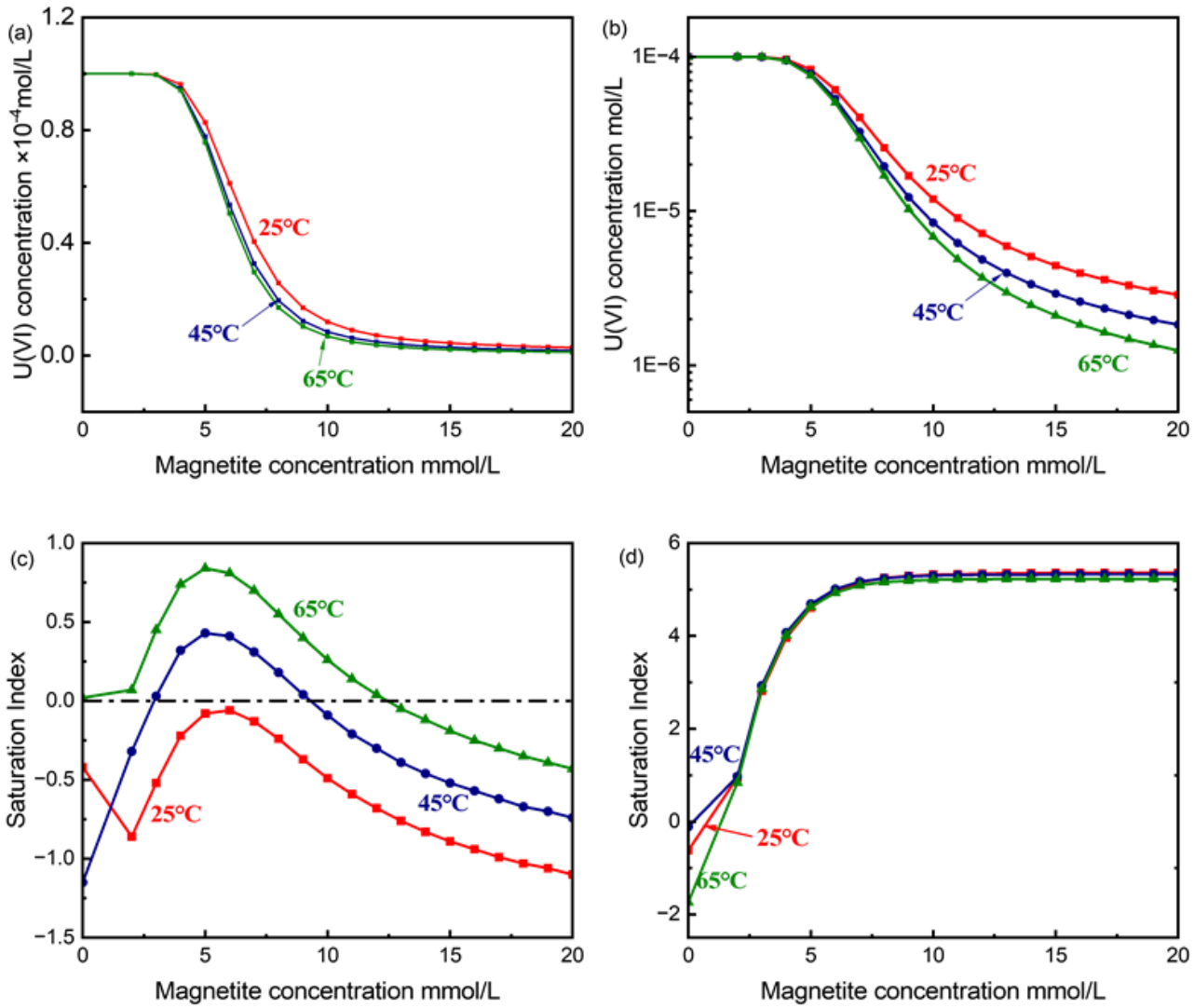


Figure 3

Effects of temperatures on uranium reduction by magnetite shown on linear (a) and logarithmic (b) coordinate axes, and effects of different temperatures on the saturation indexes of schoepite (c) and uraninite (d) (total uranium concentration: 1.0×10^{-4} mol/L)

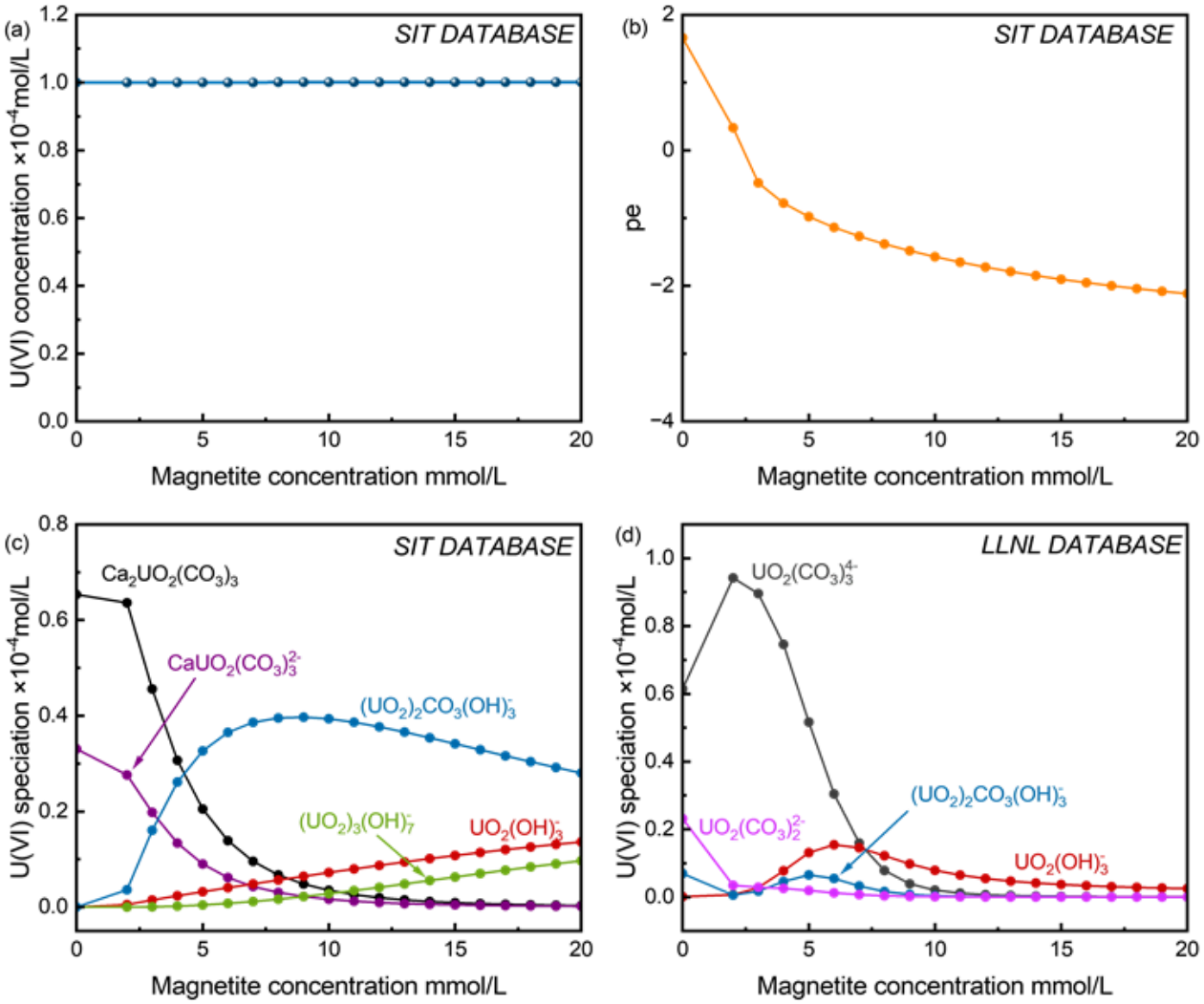


Figure 4

U(VI) concentration (a), pe (b), and U(VI) speciation (c) with magnetite concentration calculated using the SIT database, and U(VI) speciation calculated using the LLNL database (d) (total uranium concentration: 1.0×10^{-4} mol/L)